

Peter Fischer  
Heinz Rehage

## Non-linear flow properties of viscoelastic surfactant solutions

Received: 11 June 1996  
Accepted: 23 September 1996

This paper is dedicated to  
Prof. Dr. Hanswalter Giesekus in honor  
of his outstanding contributions to  
fundamental rheological research

Dr. P. Fischer (✉)<sup>1</sup> · H. Rehage  
Institut für Umweltanalytik  
Universität-Gesamthochschule Essen  
Universitätsstraße 3  
45141 Essen, Germany  
peterfischer@uni-essen.de

<sup>1</sup> Present address:  
Department of Chemical Engineering  
Stanford University  
Stanford, California 94305-5025, USA  
pf@rio.stanford.edu

**Abstract** This paper gives a quantitative description of the viscoelastic properties of aqueous solutions of entangled rod-shaped micelles. The experimental data are compared with the theoretical predictions of a special constitutive equation which is based on the concept of deformation-dependent tensorial mobility. In the regime of small deformations, shear stresses or shear rates, the dynamic features of the viscoelastic solutions are characterized by the equations of a simple Maxwell material. These phenomena are linked to the average lifetime of the micellar aggregates and the rheological properties are controlled by kinetic processes. At these conditions one observes simple scaling laws and linear relations between all rheological quantities. At elevated values of shear stresses or deformations, however, this simple model fails and non-linear properties as normal stresses, stress overshoots or shear-thinning properties occur. All these phenomena can be described by a constitutive equation which

was first proposed by H. Giesekus. The experimental results are in fairly good agreement with the theoretical predictions, and this model holds for a certain, well defined value of the mobility factor  $\alpha$ . This parameter describes the anisotropic character of the particle motion. In transient and steady-state flow experiments we always observed  $\alpha = 0.5$ . Especially at these conditions, the empirically observed Cox-Merz rule, the Yamamoto relation and both Gleißle mirror relations are automatically derived from the Giesekus model. The phenomena discussed in this paper are of general importance, and can be equally observed in different materials, such as polymers or proteins. The viscoelastic surfactant solutions can, therefore, be used as simple model systems for studies of fundamental principles of flow.

**Key words** Viscoelastic surfactant solution – non-linear flow – Giesekus model

### Introduction

Rheological constitutive equations proposed for viscoelastic materials are based upon the correlations between shear stress, shear rate, and the intrinsic parameters and functions of the investigated material. The most simple

constitutive equations were proposed by Hooke and Newton several centuries ago and those defined by Voigt/Lord Kelvin and Maxwell some 130 years ago. These linear constitutive equations are defined by the linear relationship between shear stress and shear rate.

Linear constitutive equations are limited to ideal elastic solids and viscous liquids or to combinations of

these two characteristic features. The correlation coefficient between stress and deformation depends on the applied model and is defined as viscosity, elasticity or viscoelasticity. The term viscoelasticity denotes the simultaneous coexistence of viscous and elastic properties. One of the simplest models to describe viscoelastic properties is the Maxwell model. Unfortunately, all these models mentioned above are only valid in a small regime of the applied velocity gradient or other external forces.

Leaving this well-defined regime, one will experimentally observe various non-linear flow properties. The phenomenon of non-linear response was discovered at the earliest stages of rheological research. As soon as viscometers became available, many departures from Newtonian behavior were observed. The non-Newtonian behavior is of great practical interest and is intimately connected with orientation processes or structural changes that occur during flow.

A theoretical description of these properties including the so-called elastic fluids is quite complex. Several theoretical approaches such as the generalized Newtonian model, the retarded motion model and models based upon integral and differential constitutive equations have been proposed (Bird et al., 1987; Larson, 1988).

An outstanding model for viscoelastic liquids is the generalized Oldroyd-8-constant model (Oldroyd, 1958). This model is based upon the linear Maxwell model with additional assumptions and a correct tensorial development of all involved parameters. However, most of these models do not accurately fit to the experimental data (Bird et al., 1987). Giesekus now developed an elegant and applicable model based on the Oldroyd model but using a different method to describe the molecular drag coefficient (Giesekus, 1982). The basic Maxwell model was extended by a quadratic stress tensor and a mobility tensor to govern the non linearity in a more sophisticated way, as in the Oldroyd-8-constant model. The mobility tensor describes the anisotropic mechanical properties of rod-like aggregates under flow. Besides the relaxation time of the Maxwell model, Giesekus assumes a dimensionless mobility factor,  $\alpha$ , that controls the relative mobility tensor in the regime between zero and unity.

In general the constitutive equations are stated for simplification purposes in so-called one-mode cases. Here the complete motion is expressed by one single relaxation process that defines just one characteristic time constant called the relaxation time  $\lambda$ . For example, the one-mode Maxwell model shows a monoexponential stress decay after step function shear strain or shear rate experiments. This reducing of parameters is used because one-mode equations give discrete information on molecular properties, such as diffusion or orientation mechanisms. In experiments monoexponential relaxation functions are very difficult to observe. For instance, polymer liquids always show a complex multi-mode behavior. This is due to the large number of possible molecular rear-

rangements. As a consequence, direct comparison of the theoretical predictions and experimental results is not possible for solutions of entangled macromolecules.

We propose a different way by comparing the constitutive equations with experimental results obtained from viscoelastic surfactant solutions. These systems are used as simple model systems for rheological studies because they exhibit interesting flow properties. Due to the limited life-time of the micellar aggregates monoexponential relaxation functions are often observed. The dynamic features of these solutions can be described using the theoretical equations of an ideal Maxwell material. Alternatively, a modified reptation theory can be used to describe the dynamic features (Rehage and Hoffmann, 1991; Cates, 1987). However, in the regime of large velocity gradients viscoelastic surfactant solutions exhibit the same type of non-linear flow properties as observed in polymer solutions.

In this paper we use the one-mode Giesekus model to analytically describe non-linear viscoelastic flow properties (Giesekus, 1982). From this theory it is possible to calculate steady state values of the shear viscosity and the first normal stress coefficient even at elevated shear rates. We then compare these equations with experimental data for surfactant solutions. A direct comparison between theory and experiment becomes possible due to the unique properties of surfactant solutions. In addition, we compare several semiempirical relations to the Giesekus model, such as the Cox-Merz rule (Cox and Merz, 1958), the Yamamoto relation (Bird et al., 1987) and both Gleißle mirror relationships (Gleißle, 1981). These equations, although of empirical nature, allow us to calculate steady state values from transient experiments or vice versa.

---

### Maxwell model – Linear flow properties

Linear viscoelastic properties of fluids can already be described by a combination of elastic and viscous elements. In all materials that exhibit this phenomenon the particular response of a sample depends upon the time scale of observation. Under conditions where the experiment is comparatively slow, the sample will appear to be viscous rather than elastic. At very short times, however, the elastic response is the dominant response. The rheological properties of these linear viscoelastic samples are represented by simple mechanical models. In the regime of linear stress-strain relations it is assumed that the elastic properties can be described by a Hookean spring while the viscous phenomena can be represented by a Newtonian dashpot. The simplest model that can describe a viscoelastic surfactant solution is the Maxwell model. It consists of a spring and a dashpot connected in series as shown in Fig. 1 a.

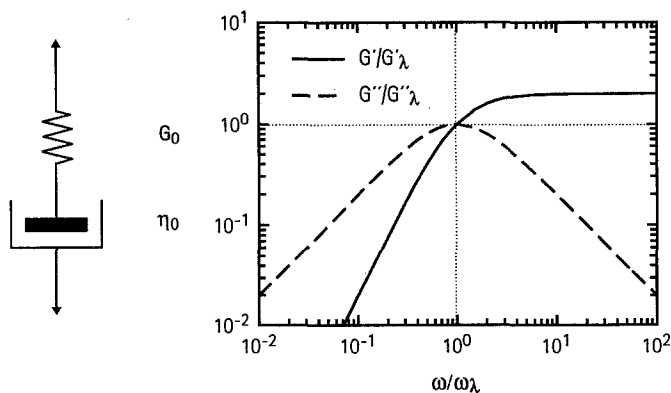


**Fig. 1A,B** Schematic representation of the Maxwell model. The elastic properties are given by the spring (relaxation modulus,  $G_0$ ) and the viscous properties are represented by the dashpot (zero shear viscosity,  $\eta_0$ ). The right drawing gives some information on the dynamic properties of the storage and loss modulus

The elastic spring corresponds to a shear modulus,  $G_0$ , and the dashpot represents the constant viscosity,  $\eta_0$ . The dynamic properties and the desired material functions of the Maxwell element can be represented by the following linear differential equation

$$\tau + \frac{\eta_0}{G_0} \frac{\partial \tau}{\partial t} = \eta \dot{\gamma} \quad (1)$$

where  $\dot{\gamma}$  denotes the shear rate,  $\tau$  is the shear stress and  $\eta$  is the viscosity. Dynamic experiments are often performed to get information on the viscoelastic properties of a solution. In this case the shear strain,  $\gamma$ , is varied periodically with a sinusoidal alternation at an angular frequency  $\omega$ . The response of the sample to the periodic change consists of a sinusoidal shear stress that is made up of two different components. The first component is in-phase with the deformation while the second one is out-of-phase with the strain.

From the phase angle,  $\delta$ , and the amplitudes of the shear stress and of the shear strain it is possible to calculate the storage modulus,  $G'(\omega, \gamma)$ , and loss modulus,  $G''(\omega, \gamma)$ , from

$$G'(\omega, \gamma) = \left( \frac{\hat{\tau}_{12}(\omega, \gamma)}{\hat{\gamma}_{12}} \right) \cos \delta \quad (2)$$

$$G''(\omega, \gamma) = \left( \frac{\hat{\tau}_{12}(\omega, \gamma)}{\hat{\gamma}_{12}} \right) \sin \delta \quad (3)$$

At low values of the deformation both dynamic moduli are only functions of the angular frequency (linear viscoelastic response). Above a certain value these functions also depend on the deformation (non-linear viscoelastic response). If a rheological function depends on two pa-

rameters one usually expects non-linear properties. The storage modulus describes the elastic properties of the sample, and the loss modulus is proportional to the viscous resistance. It is convenient to express the periodically varying functions in terms of the complex modulus,  $G^*(\omega, \gamma)$ , and the magnitude of the complex viscosity,  $|\eta^*|(\omega, \gamma)$ ,

$$G^*(\omega, \gamma) = G'(\omega, \gamma) + iG''(\omega, \gamma) \quad (4)$$

$$|\eta^*|(\omega, \gamma) = \frac{G^*(\omega, \gamma)}{i\omega} = \frac{\sqrt{G'^2(\omega, \gamma) + G''^2(\omega, \gamma)}}{\omega} \quad (5)$$

The behavior of a Maxwell material under harmonic oscillations can be obtained from Eqs. (6) and (7)

$$G'(\omega, \gamma) = G_0 \frac{\omega^2 \lambda^2}{1 + \omega^2 \lambda^2} \quad (6)$$

$$G''(\omega, \gamma) - \eta_s \omega = G_0 \frac{\omega \lambda}{1 + \omega^2 \lambda^2} \quad (7)$$

where  $\eta_s$  describes the solvent viscosity and  $\lambda$  denotes the relaxation time of the one-mode material. In the regime of linear viscoelasticity the material functions do not depend upon the deformation; as a consequence they are only functions of the angular frequency. The normalized behavior of both dynamic moduli as a function of angular frequency is shown in Fig. 1 b.

In transient experiments the Maxwell material can also be described by monoexponential relaxation processes. Although the initial extension is infinitely fast, there is a time-dependent response of the viscoelastic material that can be measured to obtain the desired rheological functions. For the Maxwell fluid an applied stress always relaxes to zero after an infinitely long period of time. For example, in a relaxation test, a step function shear strain is applied to  $t = 0$ . The resulting relaxation modulus  $G(t)$  is time-dependent as shown in Eq. (8)

$$G(t) = G_0 e^{(-t/\lambda)} \quad (8)$$

The Maxwell model describes the phenomenon of monoexponential stress relaxation and can hence be used to illustrate the dynamic properties of viscoelastic liquids. The simplicity of comparing the rheological data with the theoretical predictions of a Maxwell material is rather attractive. For example, the Maxwell model is in qualitative agreement with the dynamic properties of viscoelastic surfactant solutions as will be shown later in this paper. An excellent introduction and an extensive description of linear viscoelastic response are given in the book of N. W. Tschoegl (Tschoegl, 1989).

### Giesekus model – Non-linear flow properties

The Giesekus model is a relatively simple yet powerful way to predict non-linear flow properties. Starting from the general reptation theory, which was first introduced by de Gennes and later improved by Doi and Edwards, Giesekus followed an alternative concept of deformation-dependent tensorial mobility (de Gennes, 1979; Doi and Edwards, 1986). In the reptation model, the anisometric particles are described by the Kramers freely jointed bead-rod chain. By introducing a tensorial generalization of Stoke's law and by coupling the tensor drag coefficient and the orientation of the stiff rods between two neighboring beads, Curtiss and Bird succeeded in deriving similar equations to those derived from the reptation model (Curtiss and Bird, 1981). The Giesekus model is principally based on this fundamental idea but introduces a new tensorial drag coefficient coupled with the average state of deformation (Giesekus, 1982). Even in the first stage of the theory it became evident that this model is particularly successful at describing non-linear rheological properties such as stress overshoot in start-up experiments or non-vanishing second normal stress differences in stationary shear flow. In addition to that, a limiting shear stress was obtained at high values of the velocity gradient. As these features are often observed in solutions of entangled rod-shaped micelles, there is at least a qualitative agreement with the Giesekus model.

In order to describe the anisotropic properties of the rod-shaped particles in shear and extensional flow a relative mobility tensor,  $\beta$ , is introduced that depends on the average state of orientation. It is well known that rod-shaped micelles can be aligned by the orienting forces of a velocity gradient. As a consequence, the physical properties of the streaming solutions have an anisotropic character that becomes more and more pronounced with increasing shear rate. The non-linear response of the rheological functions is then a natural consequence of the orientation effects. The mobility tensor can be associated with both the diffusion process and the anisotropic hydrodynamic drag on the aggregates (Bird and West, 1985). In a first approximation, Giesekus assumed a linear dependence between the mobility tensor and the configuration tensor,  $C$ . Such a description includes the orientation and deformation of the supermolecular network structure that is formed by the entangled anisometric particles. In the simplest case there is only one configuration tensor controlling the anisotropic mobility (Giesekus, 1982). Giesekus proposed the following linear relationship for such a simple situation

$$\beta = 1 + \alpha(C - 1) = (1 + \alpha)1 + \alpha C \quad (9)$$

The dimensionless anisotropy factor,  $\alpha$ , describes the anisotropic character of the particle mobility. It is easy to show that  $\alpha$  attains values between zero and one. The

limiting case  $\alpha = 0$  corresponds to the isotropic motion and ultimately leads to an upper convected Maxwell material. In order to derive a deformation-dependent constitutive equation a neo-Hookean law connecting the tensor of external stresses and the configuration tensor is suggested

$$\tau = 2G\gamma = G(C - 1) \quad (10)$$

In combination with this equation an upper convected Maxwell material was used to describe the viscoelastic properties of the entangled particles

$$\beta\tau + \lambda \frac{\vartheta\tau}{\vartheta t} = 2\eta\dot{\gamma} \quad (11)$$

In comparison with Eq. (1) it is easy to see that this formula represents the general form of a non-linear Maxwell material. By combining Eqs. (9) and (11) Giesekus succeeded in deriving a constitutive law which takes into account effects of orientation and non-linear viscoelastic effects

$$[1 + \alpha(C - 1)] \cdot (C - 1) + \lambda \frac{\vartheta\tau}{\vartheta t} = 2\eta\dot{\gamma} \quad (12)$$

The Giesekus model now gives a detailed relation between rheological parameters and the relative mobility tensor by inducing the anisotropy of a streaming solution. Equation (12) is used to analyze steady shear flow, start-up flow, and cessation of steady-state flow. This equation can be used to obtain information for both simple shear flow and extensional flow. We shall not go into further details here. The interested reader is referred to the extensive papers of H. Giesekus, where this procedure is described in more detail (Giesekus, 1982).

### Steady state shear flow

For steady shear flow three Eqs. (13–15) can be derived from Eq. (12). These hold for the general case, where  $0 \leq \alpha \leq 1$ .

$$[\alpha(N_1(\infty, \dot{\gamma}) - 2N_2(\infty, \dot{\gamma})) + 1] \tau(\infty, \dot{\gamma}) = \lambda \dot{\gamma} (1 - N_2(\infty, \dot{\gamma})) \quad (13)$$

$$[\alpha(N_1(\infty, \dot{\gamma}) - 2N_2(\infty, \dot{\gamma})) + 1] N_1(\infty, \dot{\gamma}) = 2\lambda \dot{\gamma} \tau(\infty, \dot{\gamma}) \quad (14)$$

$$[1 - \alpha N_2(\infty, \dot{\gamma})] N_2(\infty, \dot{\gamma}) = \alpha \tau^2(\infty, \dot{\gamma}) \quad (15)$$

## Transient flow

For transient flow three coupled differential equations can easily be obtained from Eq. (12) by using derivations of the configuration tensor

$$\begin{aligned} \dot{\tau}(t, \dot{\gamma}) + [\alpha(N_1(t, \dot{\gamma}) - 2N_2(t, \dot{\gamma})) + 1] \tau(t, \dot{\gamma}) \\ = \lambda \dot{\gamma} (1 - N_2(t, \dot{\gamma})) \end{aligned} \quad (16)$$

$$\begin{aligned} \dot{N}_1(t, \dot{\gamma}) + [\alpha(N_1(t, \dot{\gamma}) - 2N_2(t, \dot{\gamma})) + 1] N_1(t, \dot{\gamma}) \\ = 2\lambda \dot{\gamma} \tau(t, \dot{\gamma}) \end{aligned} \quad (17)$$

$$\dot{N}_2(t, \dot{\gamma}) + [1 - \alpha N_2(t, \dot{\gamma})] N_2(t, \dot{\gamma}) = \alpha \tau^2(t, \dot{\gamma}) \quad (18)$$

## Analytical solutions

Some analytical solutions can be obtained when  $\alpha = 0.5$ .

For steady state shear flow one obtains for the shear stress, first and second normal stress difference, respectively

$$\tau(\infty, \dot{\gamma}) = \frac{G_0}{2\lambda \dot{\gamma}} (\sqrt{1 + 4\lambda^2 \dot{\gamma}^2} - 1) \quad (19)$$

$$N_1(\infty, \dot{\gamma}) = 2G_0 \left( \frac{1 - A^2}{A} \right) \quad (20)$$

$$N_2(\infty, \dot{\gamma}) = G_0(A - 1) \quad (21)$$

where  $A^2$  is denoted by

$$A^2 = \frac{\sqrt{1 + 4\lambda^2 \dot{\gamma}^2} - 1}{2\lambda^2 \dot{\gamma}^2} \quad (22)$$

Besides the rather trivial cases where  $\alpha = 0$  or  $\alpha = 1$ , it is not easy to derive an analytical solution for any arbitrary value of the anisotropy factor. It is, however, possible to solve Eqs. (13) to (15) by using numerical approximations. This is rather simple because there are three equations with the same number of unknown variables. Numerical solutions can easily be obtained by the Bisection-Method, Newton's-Method, Regula-Falsi or the Secant-Method. We shall not go into further details at this point. The interested reader is referred to standard mathematics books where all these procedures are described in more detail.

For dynamic processes, such as start-up flow or relaxation after cessation of steady-state flow, one has to solve the entire set of three coupled differential equations given by Eqs. (19) to (21). Although it is possible to get analytical solutions for some special values of the mobility factor, the corresponding equations are rather complicated and not practical to use. Again, it is rather simple

to solve these non-linear differential equations by numerical computer programs for any arbitrary value of alpha. This can be done by the Euler-Cauchy method or by Runge-Kutta computer programs. The same analysis was already done by Giesekus many years before, and his calculated values are in excellent agreement with our numerical solutions. An extensive discussion of the time-dependent shear stress and normal stress differences is summarized in several publications by H. Giesekus (Giesekus, 1982, 1984, 1985, 1986).

## Semiempirical relations

There are several semiempirical relations that can be used to compare non-linear rheological properties with linear viscoelastic functions. Although they are empirical in nature they allow us to calculate steady-state values from transient or oscillatory shear experiments. In addition, some rheological properties may be determined over many orders of magnitude using these relations. From the Giesekus model it is easy to calculate these relations and compare these predictions with experimental results. In this paper we investigate the Cox-Merz rule, the Yamamoto relation, both Gleible mirror relations and finally the so-called Laun rule.

## Cox-Merz rule

It is often observed that the shear viscosity,  $\eta(\infty, \dot{\gamma})$ , coincides relatively well with the magnitude of the complex viscosity,  $|\eta^*(\omega, \dot{\gamma})|$ , for equal values of shear rate,  $\dot{\gamma}$ , and frequency,  $\omega$ . This phenomenon is usually known as the Cox-Merz rule as shown in Eq. (23)

$$\eta(\infty, \dot{\gamma}) = |\eta^*(\omega, 0)| \quad \text{for } \dot{\gamma} = \omega \quad (23)$$

It is evident that the Cox-Merz rule describes a relationship between linear and non-linear viscoelastic properties. This relationship seems to hold for solutions of entangled macromolecules. In the regime of small frequency and shear rate both viscosities become identical. In the region of high velocity gradients a small deviation is observed experimentally. The Giesekus model takes this behavior into account and agrees fairly well with experimental data. Using the Giesekus model one obtains a modified shear viscosity  $\eta(\infty, \dot{\gamma})$

$$\eta(\infty, \dot{\gamma}) = \frac{\eta_0}{2\lambda^2 \dot{\gamma}^2} [\sqrt{1 + 4\lambda^2 \dot{\gamma}^2} + 1] \quad (24)$$

The Cox-Merz rule holds for an anisotropy factor  $\alpha = 0.5$ . The magnitude of the complex viscosity is given by Eq. (25)

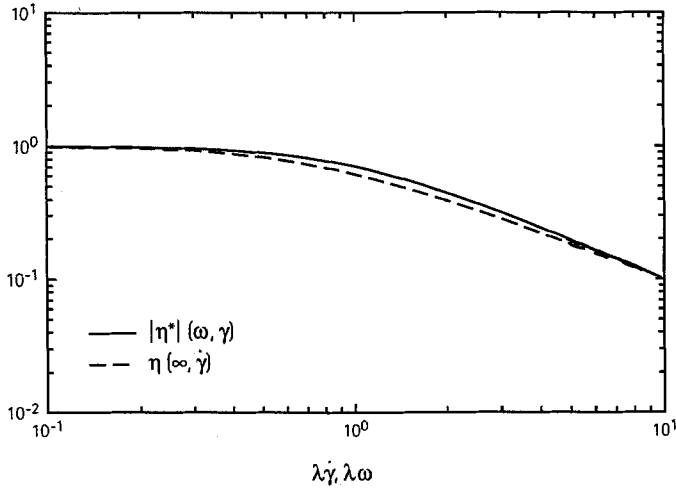


Fig. 2 Comparison of shear viscosity,  $\eta(\infty, \dot{\gamma})$ , and magnitude of the complex viscosity,  $|\eta^*(\omega, \gamma)|$ , as functions of shear rate and frequency. The curves were calculated from Eqs. (24) and (25). It is interesting to note that the difference between both functions is rather small when plotting them in logarithmic scale

$$|\eta^*(\omega, \gamma)| = \frac{\eta_0}{\sqrt{1 + \omega^2 \lambda^2}} \quad (25)$$

In Fig. 2 both viscosities are shown as function of shear rate and frequency. Although there is a small difference in a linear plot it is more difficult to recognize this deviation on a logarithmic scale. In any case, the differences between the shear viscosity and the magnitude of the complex viscosity are only small and a high precision is essential to compare theoretical results with experimental data.

### Yamamoto relation

The Yamamoto relation (Bird et al., 1987; Fischer and Rehage, 1994; Attané et al., 1985; Attané et al., 1988; Kissi et al., 1993) is often used to obtain the normal stress coefficient  $\Psi_1(\infty, \dot{\gamma})_{YM}$  from transient experiments after cessation of steady-state shear flow. According to Eq. (26) the first normal stress coefficient  $\Psi_1(\infty, \dot{\gamma})_{YM}$  is calculated from the shear stress decay function  $\eta^-(t, \dot{\gamma})$  after cessation of steady-state shear flow

$$\Psi_1(\infty, \dot{\gamma})_{YM} = 2 \int_0^{\infty} \eta^-(t, \dot{\gamma}) dt \quad (26)$$

The shear stress decay function  $\eta^-(t, \dot{\gamma})$  is calculated by dividing the shear stress by the shear rate as shown in Eq. (27)

$$\eta^-(t, \dot{\gamma}) = \frac{\tau(t, \dot{\gamma})}{\dot{\gamma}} \quad (27)$$

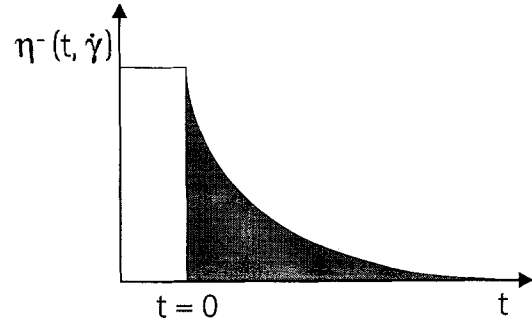


Fig. 3 Comparison of the normal stress coefficient,  $\Psi_{1n}(\infty, \dot{\gamma})_{YM}$ , and the stress decay coefficient,  $\eta^-(\infty, \dot{\gamma})$ , according to the Yamamoto relation

In Fig. 3 this method is shown graphically. The Yamamoto relation can be used to obtain the stationary values of the first normal stress coefficient  $\Psi_1(\infty, \dot{\gamma})$ . This holds in the regimes of linear and non-linear flow properties.

### Gleißle mirror relations

Both mirror relations introduced by Gleißle (Gleißle, 1980; Gleißle, 1981; Kissi et al., 1993; Fischer and Rehage, 1994) were derived from experimental observations. The relations again give some correlations between linear and non-linear flow properties. As the expression “mirror relation” suggests, one obtains non-linear functions by reflecting an appropriate linear function on the vertical axis. The first Gleißle relation correlates the shear stress growth coefficient,  $\eta^+(t, \dot{\gamma})$ , that is measured in a step function shear rate to the steady-state value shear viscosity,  $\eta(\infty, \dot{\gamma})$ . To obtain this correlation one has to plot  $\eta(\infty, \dot{\gamma})$  as a function of  $1/\dot{\gamma}$  as shown in Eq. (28)

$$\eta^+(t, \dot{\gamma}) = \eta(\infty, \dot{\gamma}) \quad \text{for} \quad t = \frac{1}{\dot{\gamma}} \quad (28)$$

The second Gleißle relation correlates the first normal stress growth coefficient,  $\Psi_1^+(t, \dot{\gamma})$ , to the steady-state value of the normal stress coefficient,  $\Psi_1(\infty, \dot{\gamma})$ . Again, one has to plot  $\Psi_1(\infty, \dot{\gamma})$  as a function of  $1/\dot{\gamma}$

$$\Psi_1^+(t, \dot{\gamma}) = \Psi_1(\infty, \dot{\gamma}) \quad \text{for} \quad t = \frac{1}{\dot{\gamma}} \quad (29)$$

The great advantage of these relationships is due to the simple correlation between the time-dependent and stationary rheological functions.

## Laun rule

The first normal stress coefficient  $\Psi_1(\infty, \dot{\gamma})$  and the storage module  $G'(\omega, \dot{\gamma})$  are related by the so-called Laun rule (Laun, 1986). It holds at low values of the angular frequency and the shear rate while at high shear rates large deviations occur. The relationship is given by

$$\lim_{\omega \rightarrow 0} \left( \frac{G'(\omega, 0)}{\omega^2} \right) = \lim_{\dot{\gamma} \rightarrow 0} \left( \frac{N_1(\infty, \dot{\gamma})}{2\dot{\gamma}^2} \right) = \lim_{\dot{\gamma} \rightarrow 0} \Psi_1(\infty, \dot{\gamma}) \quad (30)$$

As it is always very difficult to get precise data for the first normal stress difference in the linear viscoelastic regime, the Laun rule allows one to calculate these values from the measurement of the storage modulus. This is an interesting procedure to get more information on the viscoelastic properties of the investigated sample.

## Viscoelastic surfactant solutions – Rheological model system

Viscoelastic solutions are often formed by cationic surfactants and special types of counterions. Aqueous solutions of these compounds are sometimes used as simple model systems for rheological studies because of their gel-like flow properties (H. Hoffmann, 1995; Appel and Porte, 1990; Rehage and Hoffmann, 1988; Berret et al., 1993). Similar to solutions of entangled macromolecules the viscoelastic surfactant solutions may show complicated rheological properties in the regime of large velocity gradients. One generally obtains stress overshoot in start-up flow experiments and shear-thinning behavior as well as first normal stress differences (Fischer and Rehage, 1995; Kathory et al., 1993).

In contrast to polymer solutions, entangled networks of rod-shaped micelles exhibit much simpler rheological behavior. At low concentrations, when the lengths of the rods are much smaller than their mean distance of separation, there exists a sol state that is highly sensitive to shear forces. At higher surfactant concentrations, where the sizes of the rod-shaped micelles become comparable to their mean distance of separation, one observes gel formation and the solutions exhibit pronounced elastic properties. These elongated, rod-shaped micelles are strongly entangled. In comparison to solutions of macromolecules, there is, however, one important difference. The anisometric aggregates of surface-active compounds are in thermal equilibrium with single monomers. The permanent exchange of surfactant molecules leads to reversible breakage and reforming of the aggregates which has important consequences on the stress relaxation mechanism. This kinetic phenomenon leads to a finite lifetime of the anisometric micelles. In situations

where the elongated micelles are breaking within the time scale of observation, the rheological properties are controlled by kinetic processes. It is only under these circumstances that we obtain very simple scaling laws and linear relations between all rheological quantities. The dynamic features of these entangled micelles alternatively can be characterized by a modified reptation theory (de Gennes, 1979; Doi and Edwards, 1986; Cates, 1987; Turner and Cates, 1992; Cates, 1994). This theory involves the conventional reptation model for polymers and a special theory describing the reversible scission and recombination of micellar aggregates. In the fast breaking regime, where the average lifetime of the micelles is much shorter than the timescale of reptation ( $\lambda_{\text{BREAK}} \ll \lambda_{\text{REP}}$ ) one obtains monoexponential stress relaxation functions. This phenomenon leads to the theoretical equations of the formerly discussed Maxwell model. According to the theory of M. Cates the relaxation time,  $\lambda$ , of the one-mode Maxwell fluid is now given by

$$\lambda = \sqrt{\lambda_{\text{BREAK}} \lambda_{\text{REP}}} \quad (31)$$

Different kinds of molecular motion, breaking mechanisms, and more detailed information concerning the kinetic time constants and their influence on the flow behavior have already been discussed in several papers (Cates and Candau, 1990; Rehage and Hoffmann, 1991; Turner and Cates, 1992).

## Experiment

The rheological experiments were performed using a Rheometrics Fluid Spectrometer RFS II (0.02 rad cone-plate geometry, 50 mm,  $T = 20^\circ\text{C}$ ). The investigated angular frequency range was 0.01 to 100 rad/s. The cone-plate geometry allows one to apply shear rates between 0.05 and  $5000\text{ s}^{-1}$ . The angular frequencies and shear rates cover the regimes of both linear and non-linear flow properties of the investigated solutions. To avoid evaporation, a special solvent trap was used during the experiments.

For all rheological tests, solutions of 60 mmol/L Cetyltrimethylammonium Bromide and 350 mmol/L Sodium Salicylate (CTAB-NaSal 60-350) and 100 mmol/L Cetylpyridinium Chloride and 250 mmol/L Sodium Salicylate (CPyCl-NaSal 100-250) were used.

A systematic error of 3%, due to the inaccuracy of measuring time, normal forces and torque, is assumed to hold for all rate and frequency sweep experiments. Due to the electronic lag time of the torque transducer and the inertia of all mechanical parts a calibration was performed with Newtonian fluids of the same viscosity as the investigated surfactant solution.

## Results and discussion

We have systematically investigated the linear and non-linear rheological behavior of viscoelastic surfactant solutions in oscillatory shear flow, steady state shear flow, start-up flow and cessation of flow experiments. We compare the experimental data with the theoretical predictions of the Giesekus model. For comparison purposes we normalized all data by different methods not mentioned here in full detail (Fischer and Rehage, 1995; Fischer, 1995).

### Oscillatory experiments

A typical strain-sweep experiment of viscoelastic surfactant solutions is plotted in Fig. 4. The linear viscoelastic regime is denoted by constant rheological properties as a function of the applied strain. It is easy to recognize that the supermolecular network structures can be stretched to a limit of about 100%, before non-linear properties occur. This value is typical for the existence of rubber-like viscoelastic properties.

In dynamic experiments the flow behavior is investigated as a function of angular frequency as shown in Fig. 5. The experimental data can be qualitatively described by the relations for a Maxwell material given by Eqs. (6) and (7) (lines in Fig. 5). The relaxation time can be calculated from the intersection of  $G'(\omega, \gamma)$  and  $G''(\omega, \gamma)$ . From the experimental data one obtains  $\lambda = 0.7 \pm 0.1$  s and a relaxation modulus  $G_0 = 21.4 \pm 1.3$  Pa.

The monoexponential stress decrease can also be observed from measurements of the relaxation modulus,  $G(t)$ , as shown in Fig. 6. The relaxation modulus is measured after applying a step function shear strain. The

drawn line corresponds to predictions for a Maxwell model (Eq. (8)) and gives the same relaxation time as obtained from the dynamic measurements. The zero shear viscosity,  $\eta_0$ , can be calculated from the magnitude of the complex viscosity,  $|\eta^*(\omega, \gamma)|$ , at infinite small strains and frequencies.

### Steady-state shear flow

From steady-state shear flow experiments one obtains the shear viscosity,  $\eta(\infty, \dot{\gamma})$ , and the first normal stress difference,  $N_1(\infty, \dot{\gamma})$ , as shown in Fig. 7. For comparison purposes we introduce several dimensionless variables:

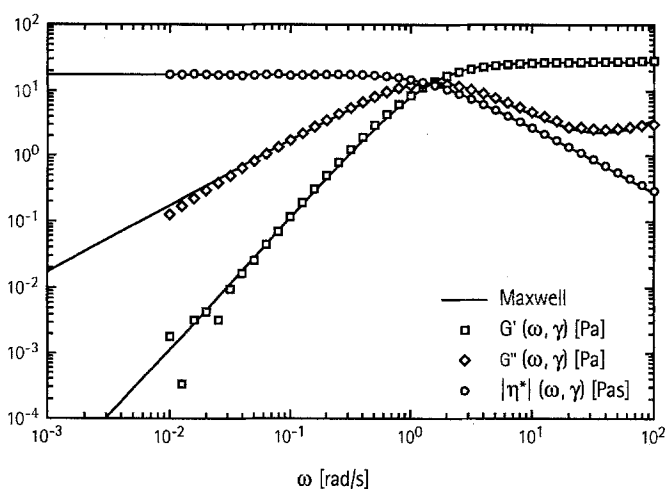


Fig. 5 Dynamic properties (dots) as a function of angular frequency,  $\omega$ , compared to the Maxwell model (lines: Eqs. (6) and (7)) ( $\gamma = 10\%$ ,  $T = 20^\circ\text{C}$ , CTAB-NaSal 60-350)

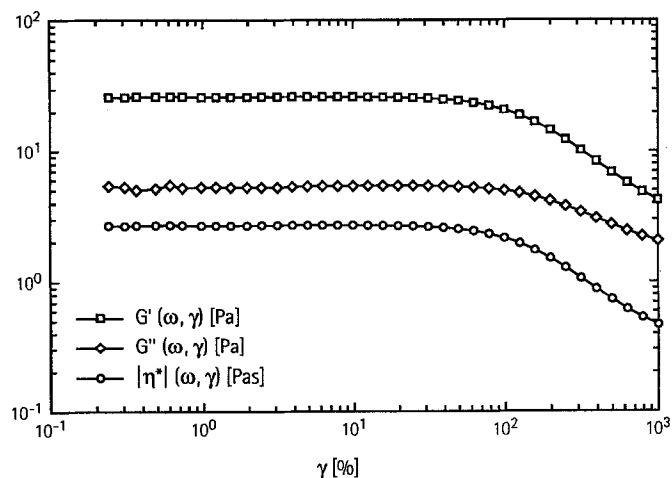


Fig. 4 Dynamic properties as a function of the deformation,  $\gamma$  ( $\omega = 10$  rad/s,  $T = 20^\circ\text{C}$ , CTAB-NaSal 60-350)

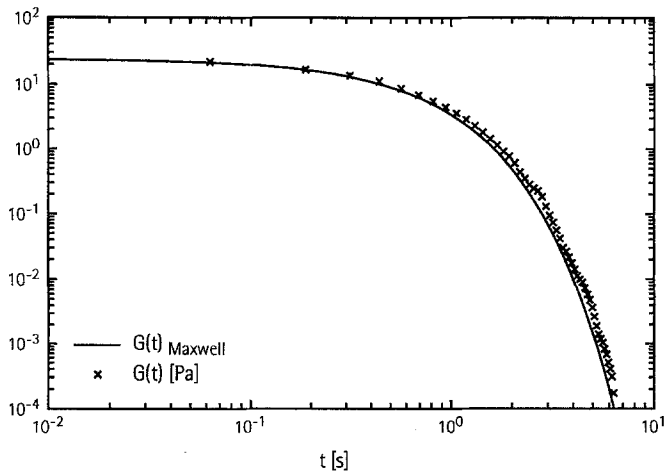
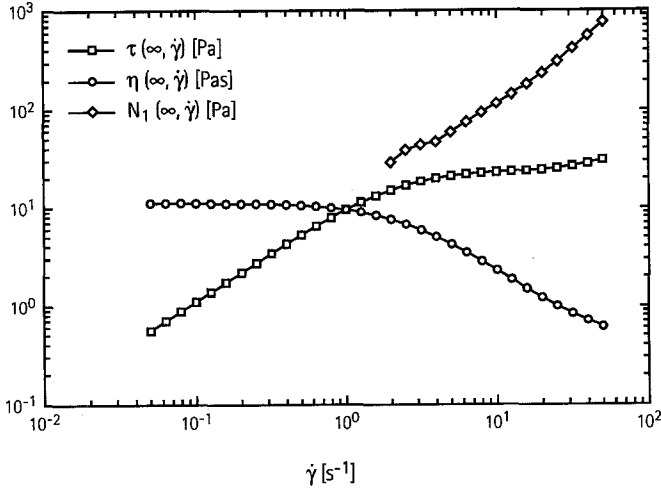


Fig. 6 Relaxation modulus (dots) as a function of time compared to the Maxwell model (lines) ( $\gamma = 20\%$ ,  $T = 20^\circ\text{C}$ , CTAB-NaSal 60-350)





**Fig. 7** Steady-state values of the shear stress,  $\tau(\infty, \dot{\gamma})$ , viscosity,  $\eta(\infty, \dot{\gamma})$ , and first normal stress difference,  $N_1(\infty, \dot{\gamma})$ , as a function of shear rate,  $\dot{\gamma}$  ( $T = 20^\circ\text{C}$ , CTAB-NaSal 60-350)

The normalized shear rate,  $\chi$ , is given by  $\lambda \dot{\gamma}$  while the normalized frequency,  $\zeta$ , is given by  $\lambda \omega$ . The investigated rheological functions are normalized by several methods not mentioned here. In general, all functions are divided by the plateau values which occur in the linear viscoelastic regime. In this way, the rheological functions are dimensionless and reduced to the value of one at infinitely low shear rates or angular frequencies. For example, the shear viscosity is divided by the zero shear viscosity and the first normal stress coefficient is divided by  $2\eta_0\lambda$ . A detailed treatment of this normalization process is given in several papers (Giesekus, 1982; Fischer, 1995). The nor-

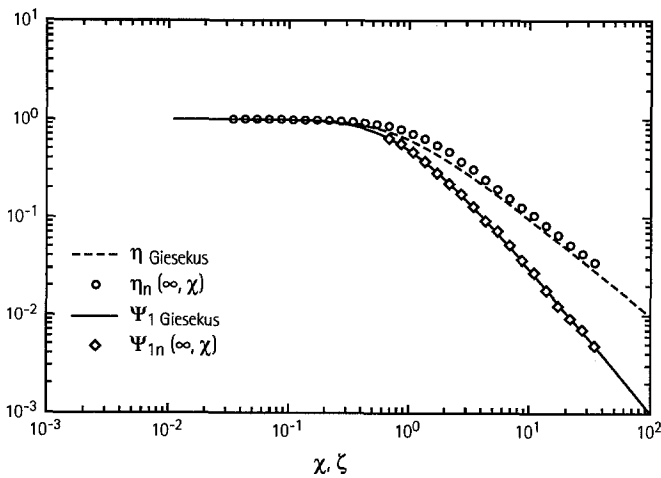


**Fig. 8** Normalized shear viscosity,  $\eta_n(\infty, \chi)$ , and first normal stress coefficient,  $\Psi_{1n}(\infty, \chi)$ , as a function of normalized shear rate,  $\chi$ , compared to the theoretical predictions of the one-mode Giesekus model (lines) ( $T = 20^\circ\text{C}$ , CTAB-NaSal 60-350)

malized results of frequency sweeps and steady-shear flow experiments with the theoretical predictions of the Giesekus model are compared in Fig. 8. Relatively good agreement between experimental results and the theoretical predictions is only obtained when the anisotropy factor is 0.5. It is interesting to note that at these conditions the Cox-Merz rule automatically is obtained from the Giesekus model. In Fig. 9 we therefore compare the magnitude of the complex viscosity,  $|\eta^*|(\omega, \lambda)$ , with the steady-state shear viscosity,  $\eta(\infty, \dot{\gamma})$ . Within the limits of experimental error we see very good agreement of the theoretical predictions of the Giesekus model and the experimental data.

In Fig. 10 the first normal stress coefficient,  $\Psi_1(\infty, \dot{\gamma})$ , obtained from rate sweep experiments, is compared to the first normal stress coefficient,  $\Psi_1(\infty, \dot{\gamma})_{YM}$ , that was calculated from relaxation experiments after cessation of steady-state shear flow as described by Eq. (26). A very good correlation of the Yamamoto relation with the theoretical predictions of the Giesekus model is obtained again by keeping the anisotropy factor  $\alpha = 0.5$ .

The first normal stress coefficient,  $\Psi_1(\infty, \dot{\gamma})$ , and the storage module,  $G'(\omega, \dot{\gamma})$ , are related by the Laun rule. As expected by the theories both functions coincide in the linear viscoelastic regime and deviate at elevated values of the shear rates. This is clearly shown in Fig. 11 where the normalized elasticity coefficient,  $G'/\zeta_n^2$ , and the normalized first normal stress coefficient,  $\Psi_{1n}(\infty, \dot{\gamma})$ , are compared to the theoretical predictions of the Giesekus model.

Here it is worthwhile to mention an extended model to predict non-linear behavior that was recently developed

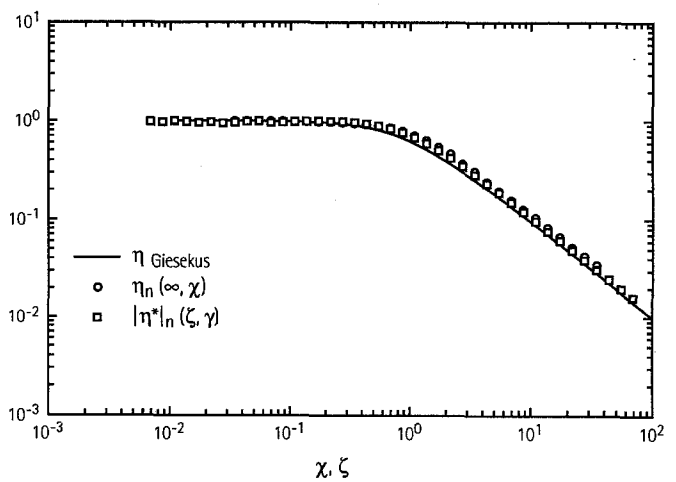


**Fig. 9** Normalized shear viscosity,  $\eta_n(\infty, \chi)$ , compared to the magnitude of the complex viscosity,  $|\eta^*|_n(\zeta, \dot{\gamma})$ , as a function of normalized angular frequency,  $\zeta$ , and shear rate,  $\chi$ . The curves clearly show that the Cox-Merz rule is applicable in the limits mentioned in Eqs. (23) and (24) ( $T = 20^\circ\text{C}$ , CTAB-NaSal 60-350)

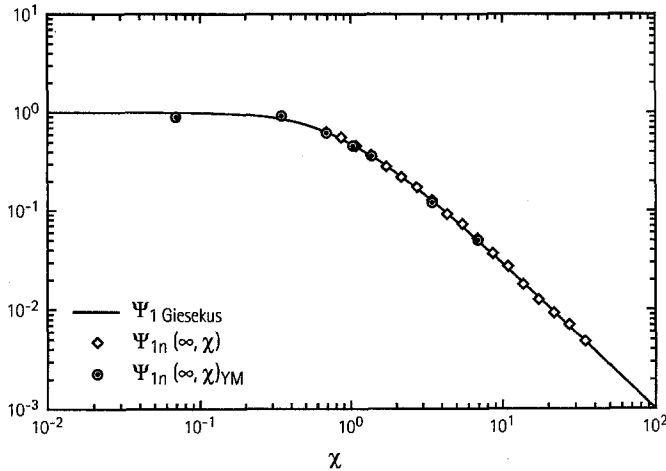


**Fig. 10** Normalized first normal stress coefficient,  $\Psi_{1n}(\infty, \chi)_{YM}$ . Calculated from the Yamamoto relation and first normal stress coefficient,  $\Psi_{1n}(\infty, \chi)$ , as a function of normalized shear rate,  $\chi$ , compared to the theoretical prediction of the one-mode Giesekus model (line) ( $T = 20^\circ\text{C}$ , CTAB-NaSal 60-350)

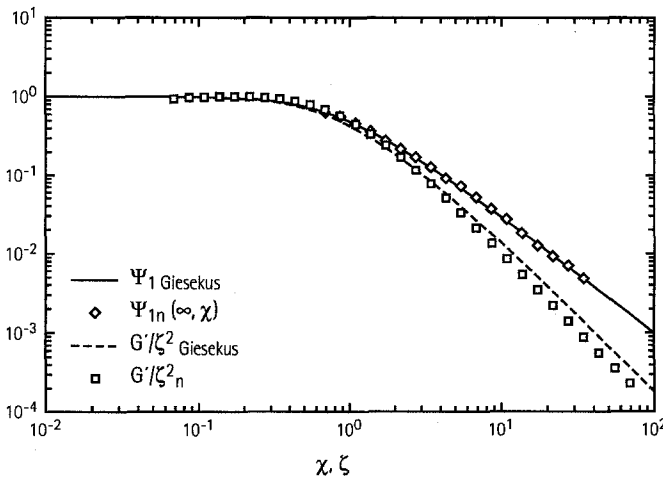


**Fig. 11** Normalized elasticity coefficient,  $G'/\zeta^2$ , and first normal stress coefficient,  $\Psi_{1n}(\infty, \chi)$ , as a function of normalized angular frequency,  $\zeta$ , and shear rate,  $\chi$ , compared to the theoretical predictions of the one-mode Giesekus model (lines). It is evident that both curves show a constant plateau level in the linear viscoelastic regime ( $T = 20^\circ\text{C}$ , CTAB-NaSal 60-350)

by Spenley and Cates (Spenley, 1994; Spenley et al., 1993). This model can be used to describe the shear and normal stress for unbreakable chains in the regime of large shear rates (Cates et al., 1993; Cates, 1990). Further, this model is used to describe the spurt effect in viscoelastic surfactant solutions (Spenley et al., 1996; Callaghan et al., 1996). It turns out that the theoretical predictions are in a fairly good agreement with experimental data only for a certain concentration regime of surfactant solutions. Vice versa, the Giesekus model is valid only in another

concentration regime. In this section we shortly outline where the theories are valid (Fischer and Rehage, 1996). As a consequence, one should keep in mind that two different models might be necessary to explain the non-linear rheology of surfactant solutions.

The theory by Cates and Spenley is based upon the entanglement theory and introduced in particular a tensorial second moment of the orientation distribution function for the tube segments. Further, the micellar break and recombination process is taken into account. In addition to the modified reptation theory mentioned above two other assumptions must be fulfilled. First the shear rate must be much larger than the average lifetime,  $\lambda_{\text{BREAK}}$ , of the rod-shaped micelles. Secondly, it is assumed that flow field does not influence the micellar aggregation process so the shear rate has no direct influence on the micellar kinetics. As a consequence, the average lifetime,  $\lambda_{\text{BREAK}}$ , is independent of the shear rate,  $\dot{\gamma}$  (Cates et al., 1993).

This theory was compared to experimental data for 100 mmol/L Cetylpyridinium Chloride with 60 mmol/L Sodium Salicylate (Rehage and Hoffmann, 1991). The investigated viscoelastic surfactant solution shows a maximum shear stress at the beginning of the non-linear regime. This shear rate is denoted as  $\dot{\gamma}_1$ . As the shear rate increases one obtains a constant but slightly unstable region in the shear stress. At very high shear rates,  $\dot{\gamma}_2$ , a second upturn in the shear stress is indicated. In Fig. 12 a recent rate sweep experiment of this viscoelastic surfactant solution is shown. We have, in addition, plotted the first normal stress difference here. It is worthwhile to mention this because it shows a similar behavior to the shear stress. In addition by simply looking at the sample we observe that the solution turns from the former sample to the more inhomogeneous structures at higher shear

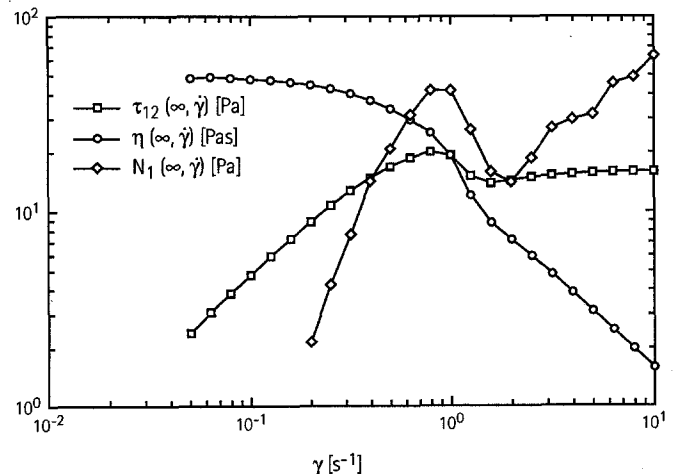


**Fig. 12** Shear stress,  $\tau(\infty, \dot{\gamma})$ , viscosity,  $\eta(\infty, \dot{\gamma})$ , and first normal stress difference,  $N_1(\infty, \dot{\gamma})$ , as a function of shear rate,  $\dot{\gamma}$  ( $T = 20^\circ\text{C}$ , CPyCl-NaSal 100-60)

rates. In the regime of shear rates  $\dot{\gamma}_1 > \dot{\gamma} > \dot{\gamma}_2$  Cates predicts a shear-banding effect (spurt effect). The flow instability and the turnup of shear stress can be described by the spurt effect (Spenley et al., 1996; Callaghan et al., 1996).

From recent data we can conclude that this behavior is restricted to a narrow regime of the counterion concentration. The unstable flow regime is indicated by the solid line in Fig. 13 where the zero shear viscosity,  $\eta_0$ , is plotted as a function of the counterion concentration (from Rehage and Hoffmann, 1991, Fig. 13). Leaving this region by increasing the counterion concentrations one obtains much simpler rheological data as shown in Fig. 7. From a counterion concentration of 200 mmol/L and above we obtain smooth curves and no shear-banding effect. This is exactly the concentration regime, where the Giesekus model holds.

Some simple relationships between linear and non-linear rheological properties are predicted by Cates at conditions, where the spurt effect occurs (Cates et al., 1993). One correlation is based on the relationship between the steady value of the shear stress,  $\tau_{\text{plateau}}$ , in the regime  $\dot{\gamma}_1 > \dot{\gamma} > \dot{\gamma}_2$  and the plateau modulus obtained from dynamic experiments. The exact correlation is given in Eq. (32)

$$\frac{\tau_{\text{plateau}}}{G_0} = 0.67 \quad (32)$$

Furthermore, the critical shear rate  $\dot{\gamma}_1$  is related to the relaxation time  $\lambda$  by

$$\lambda \dot{\gamma}_1 = 2.6 \quad (33)$$

We tested both equations for several surfactant systems (Fischer and Rehage, 1996). In Fig. 14 the ratio  $\tau_{\text{plateau}}/G_0$  is plotted as function of the counterion concentration.

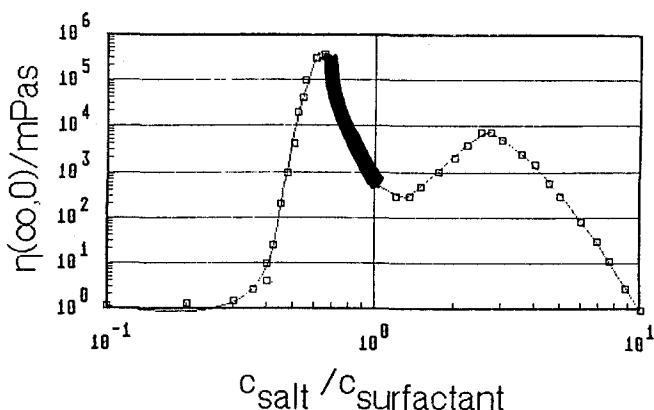


**Fig. 13** Zero shear viscosity,  $\eta_0$ , of a solution of 100 mmol/L Cetylpyridinium Chloride as function of added Sodium Salicylate concentration (from Rehage and Hoffmann, 1991)

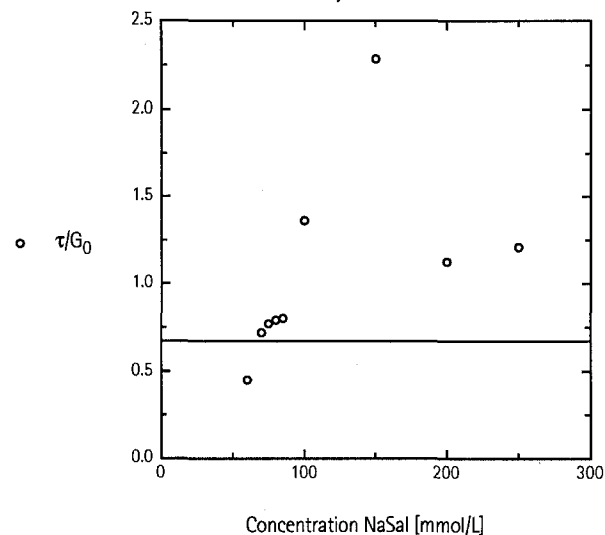


**Fig. 14** Ratio  $\tau_{\text{plateau}}/G_0$  as a function of added Sodium Salicylate concentration ( $T = 20^\circ\text{C}$ , 100 mmol/L Cetylpyridinium Chloride)

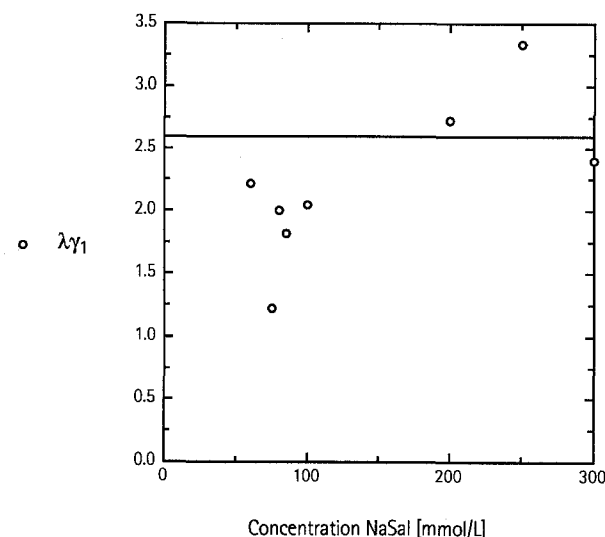


**Fig. 15** Critical shear rate  $\lambda \dot{\gamma}_1$  as a function of added Sodium Salicylate concentration ( $T = 20^\circ\text{C}$ , 100 mmol/L Cetylpyridinium Chloride)

centration. The solid line indicates the theoretical prediction of 0.67. It is easy to see that in the concentration regime between 50 and 85 mmol/L Sodium Salicylate the experimental results approximately coincide with the theory, while at higher concentrations large deviations occur. In Fig. 15 the ratio  $\lambda \dot{\gamma}_1$  is plotted as a function of counterion concentration. Here the results show even more deviation, but one might state they are on the same order of magnitude as predicted by theory. By testing several surfactant solutions at different concentrations we

found only narrow regimes where both predictions seem to hold (Fischer and Rehage, 1996).

At elevated values of the counterion concentration, all these effects disappear and simpler rheological properties can be obtained. From Eq. (24) it is easy to see that there is a plateau value of the shear stress at high values of the velocity gradient. For the both surfactant solutions investigated here the plateau value is equal to the zero-shear modulus  $G_0$ . Such a behavior is shown in Fig. 7. By comparison with measurements of the relaxation modulus in Fig. 6 and with dynamic measurements in Fig. 5 it is easy to see that the plateau value of the shear stress  $\tau = 22.0$  Pa coincides pretty well with the zero shear modulus  $G(t) = 21.4$  Pa. It is also clear from Fig. 14 that this special behavior is only valid at counterion concentrations above 200 mmol/L.

### Transient experiments

In transient tests a stepwise transition is used from one equilibrium state to another. In these experiments a certain shear stress  $\tau$ , a certain deformation  $\gamma$  or a certain shear rate  $\dot{\gamma}$  is suddenly applied at  $t = 0$  and then held constant thereafter. Although the initial extension is infinitely fast, there is a certain time response of the viscoelastic material that can be measured to obtain the desired rheological functions. From these data, viscoelastic parameters can be evaluated.

### Start-up flow

In the start-up flow tests, a step function shear rate is applied at  $t = 0$ . The resulting stress is time-dependent, and this quantity is measured after the deformation has occurred. In this case, the shear stress is measured as a function of time and the shear stress growth coefficient,  $\eta^+(t, \dot{\gamma})$ , can be calculated by Eq. (34)

$$\eta^+(t, \dot{\gamma}) = \frac{\tau(t, \dot{\gamma})}{\dot{\gamma}} \quad (34)$$

In viscoelastic solutions, the shear stress growth coefficient is exponentially increasing. It is easy to show that the time derivative of  $\eta^+(t, \dot{\gamma})$  gives the relaxation modulus

$$G(t, \dot{\gamma}) = \frac{d\eta^+(t, \dot{\gamma})}{dt} \quad (35)$$

The normalized results of transient start-up shear flow experiments and the predictions of the Giesekus model are compared in Figs. 16 to 19. In these experiments the applied steady shear rate is increased systematically from 0.1 to 25 s<sup>-1</sup>. In the regime of linear flow properties one

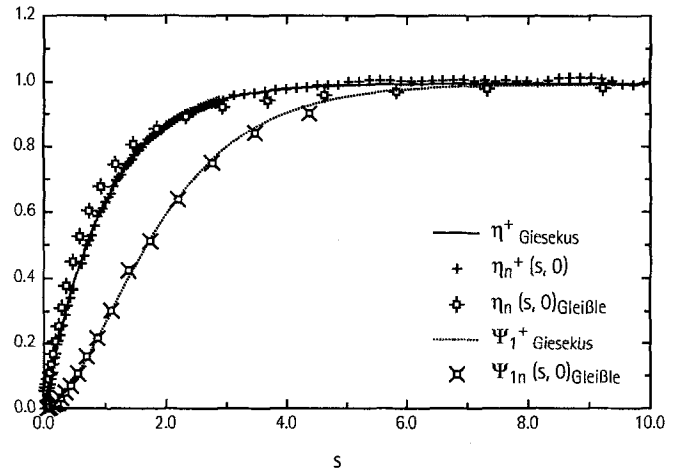


Fig. 16 Normalized stress growth coefficient,  $\eta_n^+(s, 0)$ , first normal stress growth coefficient,  $\Psi_{1n}^+(s, 0)$ , reflected shear viscosity,  $\eta(\infty, \dot{\gamma})$ , and reflected first normal stress coefficient,  $\Psi_{1n}(\infty, \dot{\gamma})$  (Gleißle relation) as a function of the normalized time,  $s$ , compared to the theoretical predictions of the one-mode Giesekus model (lines) ( $T = 20^\circ\text{C}$ , CTAB-NaSal 60-350)

observes a monoexponential increase of the shear stress growth coefficient whose plateau value is equal to the zero shear viscosity. Due to the very small first normal stress difference in the regime of linear viscoelastic response, as shown in Fig. 16, it is difficult to get precise experimental data for this rheological property. At high values of the shear rate, where non-linear flow properties occur, a complex behavior is observed.

An overshoot in the shear stress and normal stress becomes increasingly significant with increasing the shear rate, as shown in Figs. 17 to 19. In comparison to the

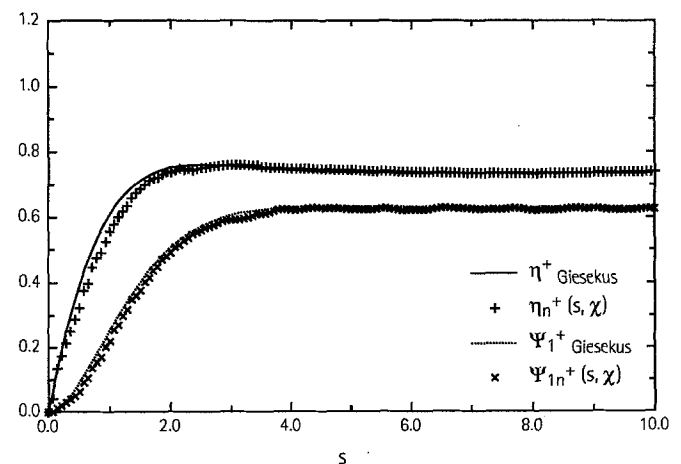
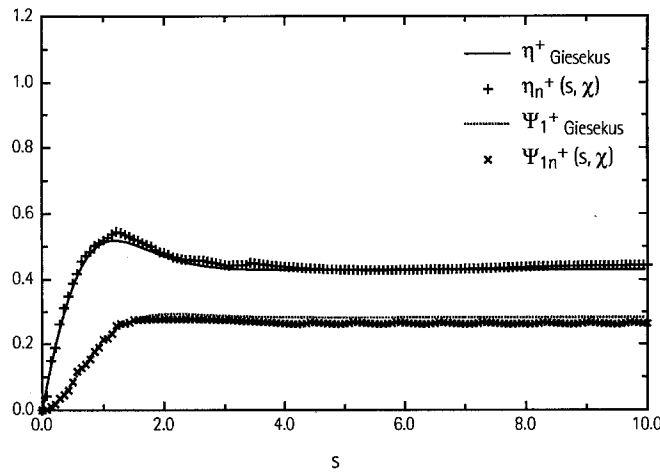


Fig. 17 Normalized stress growth coefficient,  $\eta_n^+(s, \dot{\gamma})$ , and first normal stress growth coefficient,  $\Psi_{1n}^+(s, \dot{\gamma})$ , as a function of the normalized time,  $s$ , at a shear rate  $\dot{\gamma} = 10 \text{ s}^{-1}$  compared to the theoretical predictions of the one-mode Giesekus model (lines) ( $T = 20^\circ\text{C}$ , CPyCl-NaSal 100-250)

linear regime the steady-state values of both functions are much smaller. Very good agreement between the experimental data and the theoretical predictions of the Giesekus model is obtained by keeping the anisotropy factor,  $\alpha = 0.5$ . In Table 1 the relevant steady-state values are shown for both investigated surfactant solutions. For comparison purposes, the theoretical values of the Giesekus model are also summarized and it is evident that

**Table 1** Normalized steady-state values of the shear stress growth coefficient and the first normal stress growth coefficient for each investigated surfactant solution. The experimental results are compared to the theoretical predictions

Systems & shear rate $\dot{\gamma}$ [s <sup>-1</sup> ]	Normalized growth coefficients				
	$\eta_n^+(\infty, \zeta)$	$\eta_{\text{Giesekus}}^+$	$\Psi_{1n}^+(\infty, \zeta)$	$\Psi_{1\text{Giesekus}}^+$	
CTAB-NaSal 0.1	1.00 ± 0.02	1.00	—	1.00	
60-350 10	0.14 ± 0.02	0.14	0.05 ± 0.01	0.05	
CPyCl-NaSal 10	0.73 ± 0.02	0.73	0.65 ± 0.05	0.63	
100-250 25	0.43 ± 0.02	0.43	0.28 ± 0.05	0.28	



**Fig. 18** Normalized stress growth coefficient,  $\eta_n^+(s, \chi)$ , and first normal stress growth coefficient,  $\Psi_{1n}^+(s, \chi)$ , as a function of the normalized time,  $s$ , at a shear rate  $\dot{\gamma} = 25 \text{ s}^{-1}$  compared to the theoretical predictions of the one-mode Giesekus model (lines) ( $T = 20^\circ\text{C}$ , CPyCl-NaSal 100-250)

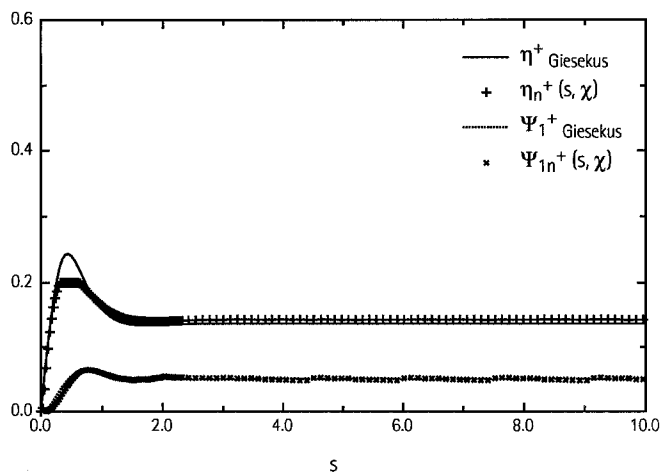


**Fig. 19** Normalized stress growth coefficient,  $\eta_n^+(s, \chi)$ , and first normal stress growth coefficient,  $\Psi_{1n}^+(s, \chi)$ , as a function of the normalized time,  $s$ , at a shear rate  $\dot{\gamma} = 10 \text{ s}^{-1}$  compared to the theoretical predictions of the one-mode Giesekus model (lines). The discrepancy between the theoretical data and the experimental ones near the maximum are due to the overload of the torque transducer ( $T = 20^\circ\text{C}$ , CTAB-NaSal 60-350)

all experiments can be interpreted in the framework of these equations.

In addition, both Gleißle mirror relations are plotted in Fig. 16. Both the steady-state shear viscosity and first normal stress coefficient are treated as mentioned in Eqs. (28) and (29) and are further normalized so that dimensionless functions result (Fischer, 1995). It is easy to recognize that the first and second Gleißle mirror relations also hold for  $\alpha = 0.5$ .

#### Stress relaxation after cessation of flow

In another transient test the constant shear rate is suddenly reduced to zero. Again the shear stress is measured as a function of time. From this parameter the shear stress decay coefficient,  $\eta^-(t, \dot{\gamma})$ , can be calculated as shown in Eq. (27). The shear stress decay coefficient describes the stress relaxation after cessation of steadystate flow for viscoelastic samples. At time zero the decay functions start at the steady-state value and relax to zero, as shown in Figs. 20 and 21. In these experiments the applied steady shear rate is systematically increased from 5 to 15 s<sup>-1</sup>. Similar to start-up experiments, one obtains linear and non-linear flow behavior depending on the actual shear rate. The normalized results of these transient experiments are in reasonable agreement with the theoretical predictions of the Giesekus model for an anisotropy factor  $\alpha = 0.5$ .

#### Summary

In the preceding sections we have systematically investigated the non-linear flow properties of viscoelastic surfactant solutions. It turns out that the experimental results are in fairly good agreement with the theoretical prediction of the one-mode Giesekus model. This holds, however, only for an anisotropy factor of  $\alpha = 0.5$ . It is interesting to note that at this exact condition the Giesekus model coincides with another theory, which was first pro-

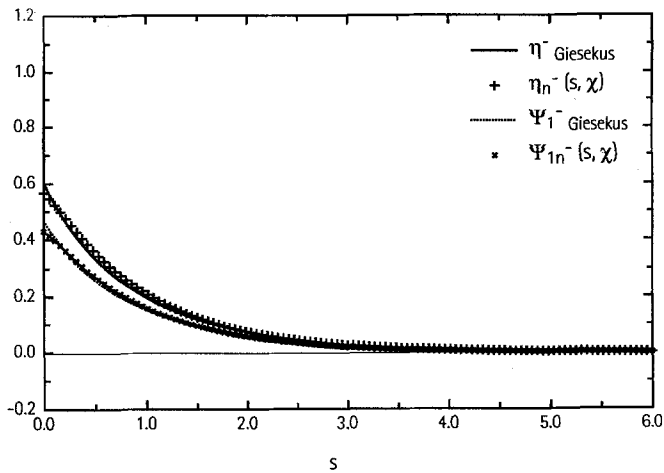


**Fig. 20** Normalized stress decay coefficient,  $\eta_n^-(s, \chi)$ , and first normal stress decay coefficient,  $\Psi_{1n}^-(s, \chi)$ , as a function of the normalized time,  $s$ , at a shear rate  $\dot{\gamma} = 15\text{ s}^{-1}$  compared to the theoretical predictions of the one-mode Giesekus model (lines) ( $T = 20^\circ\text{C}$ , CPyCl-NaSal 100-250)

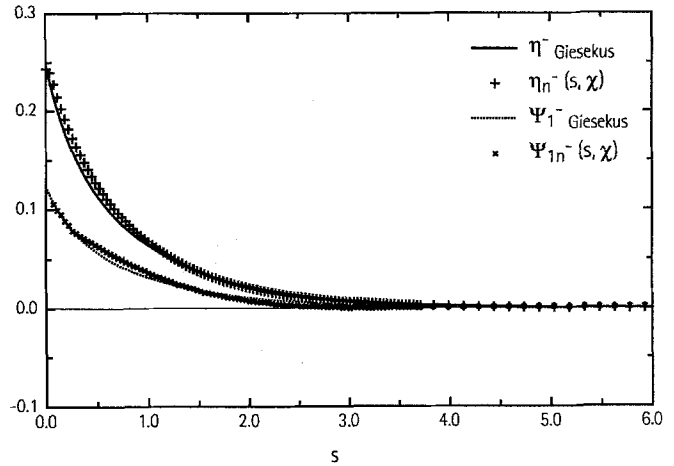


**Fig. 21** Normalized stress decay coefficient,  $\eta_n^-(s, \chi)$ , and first normal stress decay coefficient,  $\Psi_{1n}^-(s, \chi)$ , as a function of the normalized time,  $s$ , at a shear rate  $\dot{\gamma} = 5\text{ s}^{-1}$  compared to the theoretical predictions of the one-mode Giesekus model (lines) ( $T = 20^\circ\text{C}$ , CTAB-NaSal 60-350)

posed by Leonov (Leonov, 1987). This implies a general character of both types of theoretical approaches. For the special case where  $\alpha = 0.5$  some semiempirical laws such as the Cox-Merz rule, the Yamamoto relation, the Gleißler mirror relation and the Laun rule are automatically satisfied. In addition to this, a constant shear stress is observed at high values of the shear rate. In contrast to the theory of M. Cates, this phenomenon is not caused by an instable regime of flow. In conclusion, one might state that the successful application of the one-mode Giesekus model is rather attractive. It is remarkable and surprising that many features can still be described by algebraic equations. The simple relationships between all

rheological functions look particularly promising in view of the growing interest in theoretical work on complex liquids. In the future, we would like to continue our work in extensional flow and look to more concentrated surfactant solutions. At least the molecular meaning of the mentioned results are not completely clear and some further investigation is necessary.

**Acknowledgment** We gratefully acknowledge the financial support of this work by grants of the Deutsche Forschungsgemeinschaft (Re 681/4-1 and Fi 665/1-1), the European Community (CHRX-CT94-0696) and the Fonds der Chemischen Industrie. Finally, we appreciate the critical reading of the manuscript by Elizabeth K. Wheeler.

## References

- Appell J, Porte G (1990) Polymerlike behaviour of giant micelles. *Europhys Lett* 1:185–190
- Attané P, Pierrard JM, Turrel G (1985) Steady and transient shear flow of polystyrene solutions 1. *J Non-Newton Fluid Mech* 18:295–318
- Attané P, Pierrard JM, Turrel G (1985) Steady and transient shear flow of polystyrene solutions 2. *J Non-Newton Fluid Mech* 18:319–333
- Attané P, Turrel G, Pierrard JM, Carreau PJ (1988) On the use of transient data for the evaluation of integral constitutive equations. *J Rheol* 32:23–46
- Berret J-F, Appell J, Porte G (1993) Linear rheology of entangled wormlike micelles. *Langmuir* 9:2851–2854
- Bird RB, Armstrong RC, Hassager O (1987) Dynamic of polymer liquids, vol 1: Fluid mechanics. John Wiley & Sons
- Bird RB, Armstrong RC, Hassager O (1987) Dynamic of polymer liquids, vol 2: Kinetic theory. John Wiley & Sons
- Callaghan PT, Cates ME, Rofe CJ, Smeulders JBAF (1996) A study of the “spurt effect” in wormlike micelles using nuclear magnetic resonance microscopy. *J de Phys II* 6:375–393
- Cates ME (1987) Reptation of living polymers: Dynamics of entangled polymers in the presence of reversible chain-scission reactions. *Macromolecules* 20: 2289–2296
- Cates ME, Candau SJ (1990) Statics and dynamics of worm-like surfactant micelles. *J Phys: Cond Mat* 2:6869–6892
- Cates ME (1990) Nonlinear viscoelasticity of wormlike micelles. *J Physical Chemistry* 94:371–375
- Cates ME, McLeish TCB, Marrucci G (1993) The rheology of entangled polymers at very high shear rates. *Europhys Lett* 21:451–456
- Cates ME (1994) Theoretical modeling of viscoelastic phases. In: Structure and flow in surfactant solutions. ACS Symp Ser, vol 578:32–51
- Cox WP, Merz EH (1958) Correlation of dynamic and steady flow viscosities. *J Poly Sci* 619–622
- Curtiss CF, Bird RB (1981) A kinetic theory for polymer melts. *J Chem Phys* 74: 2016–2025, 2026–2033

- Doi M, Edwards SF (1986) The theory of polymer dynamics. Oxford University Press
- Fischer P, Rehage H (1994) Normalspannungsuntersuchungen an Tensidsystemen mit monoexponentiellen und „stretched exponential“ Relaxationsverhalten. DPG Symposium, Halle/Saale
- Fischer P, Rehage H (1995) Quantitative description of the non-linear flow properties of viscoelastic surfactant solutions. *Progr Col Poly Sci* 98:94–98
- Fischer P (1995) Nicht-lineare rheologische Phänomene in viskoelastischen Tensidlösungen. Wissenschaftlicher Buchverlag Dr. Fleck
- Fischer P, Rehage H (1996) in preparation
- de Gennes P-G (1979) Scaling concepts in polymer physics. Cornell University Press
- Giesekus H (1966) Die Elastizität von Flüssigkeiten. *Rheol Acta* 5:29–35
- Giesekus H (1982) A simple constitutive equation for polymer fluids based on the concept of deformation-dependent tensorial mobility. *J Non-Newt Fluid Mecha* 11:69–109
- Giesekus H (1984) Molecular theories of nonlinear VE of polymers. *Rheol Acta* 23:564
- Giesekus H (1984) On configuration-dependent generalized Oldroyd derivatives. *J Non-Newt Fluid Mecha* 14:47–65
- Giesekus H (1985) Constitutive equation for polymer fluids based on the concept of configuration-dependent molecular mobility: A generalized mean-configuration model. *J Non-Newt Fluid Mecha* 17:349–372
- Giesekus H (1986) Constitutive models of polymer fluids: Toward a unified approach. In: Trends in application of pure mathematics to mechanics. Lecture Notes in Physics. Springer Verlag
- Giesekus H (1994) Phänomenologische Rheologie. Springer Verlag
- Gleißle W (1980) In *Rheology*, vol. 2: Fluids. Plenum Press
- Gleißle W (1981) The mirror relation for viscoelastic liquids. AIChE Symposium
- Hoffmann H (1994) Viscoelastic surfactant solutions. In: Structure and flow in surfactant solutions. ACS Symp Ser, vol 578:2–31
- Khatory A, Lequeux F, Kern R, Candau SJ (1993) Linear and nonlinear viscoelasticity of semidilute solutions of wormlike micelles at high salt content. *Langmuir* 9:1456–1464
- Kissi NE, Piau JM, Attané P, Turrel G (1993) Shear rheometry of polydimethylsiloxanes: Master curves and testing of Gleißle and Yamamoto relation. *Rheol Acta* 32:293–310
- Laun HM (1986) Prediction on elastic strains of polymer melts in shear and elongation. *J Rheol* 30:459–501
- Larson RG (1988) Constitutive equations for polymer melts and solutions. Butterworths
- Leonov AI (1987) On a class of constitutive equations for viscoelastic liquids. *J Non-Newt Fluid Mecha* 25:1–59
- Oldroyd JG (1958) Non-Newtonian effects in steady motion of some idealized elasto-viscous liquids. Proceedings of the Royal Society of London A245: 278–297
- Rehage H, Hoffmann H (1988) Rheological properties of viscoelastic surfactant systems. *J Phys Chem* 92:4712–4719
- Rehage H, Hoffmann H (1991) Viscoelastic surfactant solutions; model systems for rheological research. *Molecular Physics* 74:933–973
- Spenley NA, Cates ME, McLeish TCB (1993) Nonlinear rheology of wormlike micelles. *Physical Review Letters* 71: 939–942
- Spenley NA (1994) Nonlinear rheology of micelles and polymers. PhD, University of Cambridge
- Spenley NA, Yuan XF, Cates ME (1996) Nonmonotonic constitutive laws and formation of shear-banded flows. *J de Phys II* 6:551–571
- Tschoegl NW (1989) The phenomenological theory of linear viscoelastic behavior. Springer Verlag
- Turner MS, Cates ME (1992) Linear VE of wormlike micelles: a comparison of micellar reaction kinetics. *J de Phys II* 2:503–519